Synsint Research Group

Available online at www.synsint.com

Synthesis and Sintering

ISSN 2564-0186 (Print), **ISSN** 2564-0194 (Online)

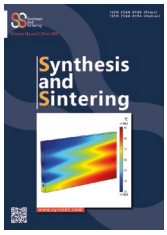

Research article

Lithium ion conductivity, crystallization tendency, and microstructural evolution of $LiZr_xTi_{2-x}(PO_4)_3$ NASICON glass-ceramics (x = 0 - 0.4)

Parisa Goharian [a], Alireza Aghaei [a], Bijan Eftekhari Yekta [b], Sara Banijamali [a,*]

[a] *Ceramic Department, Materials and Energy Research Center (MERC), Alborz, Iran*

[b] *School of Metallurgy & Materials Engineering, Iran University of Science and Technology, Tehran, Iran*

A B S T R A C T

In this research, NASICON type ($LiZr_xTi_{2-x}(PO_4)_3$) glass-ceramics were fabricated (x = 0.1, 0.2, 0.3, and 0.4). Lithium-ion conductivity along with the crystallization tendency and microstructural features were examined in this regard. Parent glasses obtained through melt quenching were converted to the glass-ceramic specimens after one-step heat treatment procedure. The resultant glass-ceramics were deeply explored by means of different techniques including scanning electron microscope, differential thermal analysis, X-ray diffractometry, and ionic conductivity measurements. According to the obtained results, presence of Zr^{4+} ions in the glass network and its gradual increase caused the enhanced crystallization temperature as well as declined crystallinity and microstructure coarsening. In all studied glass-ceramics, $LiT_2(PO_4)_3$ solid solution was the dominant crystalline phase and Zr^{4+} ions partly substituted in the structure of this crystalline phase. Moreover, presence of Zr^{4+} ions in the glass composition resulted in diminished lithium-ion conductivity of corresponded glass-ceramics at ambient temperature. Consequently, total conductivity of specimen with the highest level of ZrO_2 (x = 0.4) was measured to be 0.78×10^{-5} Scm^{-1}, being considerably less than ionic conductivity of the base (x = 0) glass-ceramic (3.04×10^{-5} Scm^{-1}). It seems that less crystallinity of ZrO_2 containing glass-ceramics decreases required connectivity between the lithium-ion free paths and is responsible for the diminished ionic conductivity of these specimens.

KEYWORDS

Glass-ceramic
Crystallization
Ionic conductivity
Zirconium ions
NASICON

OPEN ACCESS

1. Introduction

In recent decades, the increasing development of the electronic industry has necessitated the invention of new generations of energy storage materials. Among them, lithium-ion batteries have been growingly attended to thanks to their high ionic conductivity, appropriate energy density besides lightweight, and the negligible difference between the thermal expansion behavior of electrodes and electrolyte material [1–3]. Lithium titanium phosphate ceramics with the NASICON crystalline phase ($LiTi_2(PO_4)_3$) have been introduced as the remarkable electrolytes to be utilized as lithium ionic conductors in lithium-ion batteries at ambient temperature. The brilliant conductivity of NASICON ceramics stems from the special structure of the NASICON phase in which lithium ions can easily jump and transfer through two main conducting channels (A1 and A2

* Corresponding author. *E-mail address:* banijamali@merc.ac.ir, banijamalis@yahoo.com (S. Banijamali)

Received 12 March 2023; Received in revised form 2 May 2023; Accepted 8 May 2023.

https://doi.org/10.53063/synsint.2023.32148

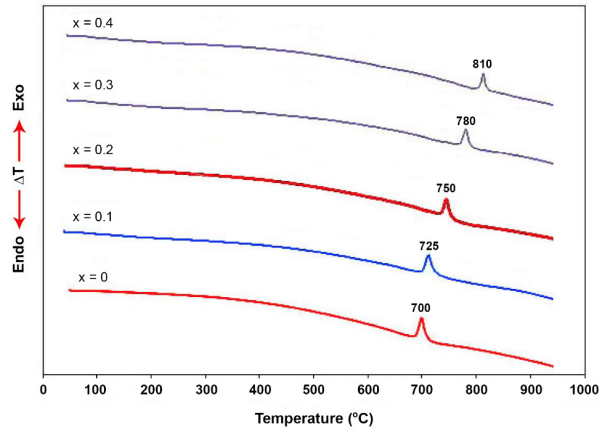

Fig. 1. DTA curves of parent glasses (heating rate: 5 °C/min).

sites). Contrary to superior ionic conductivity, these ceramics suffer from a lack of sufficient density after sintering. As a result, the remained porosity would deteriorate their ionic conductivity. Therefore, several researches have been focused on the fabrication of NASICON ceramics through the glass-ceramic route in which NASICON crystalline phase precipitates in the glass matrix under a carefully scheduled heat treatment program. NASICON type glass-ceramics can be obtained according to the desired shape and dimension without any porosity [4–10]. In different classes of NASICON type glass-ceramic, titanium ions in $LiTi_2(PO_4)_3$ crystalline phase could be partially substituted with trivalent (like Al^{3+}, La^{3+}, Cr^{3+}, and Fe^{3+}) and tetravalent (like Zr^{4+}, Hf^{4+}, Ge^{4+}, and Sn^{4+}) ions [11–14]. It is believed that by partial substitution of titanium ions by trivalent ions in the structure of the NASICON phase, ionic conductivity would be enhanced due to the enhanced number of Li^+ ions. On the other hand, the replacement of titanium ions with tetravalent ions in the NASICON structure reinforces the chemical resistance of the corresponding electrolyte against the lithium electrode and keeps titanium ions as Ti^{4+} without reduction to Ti^{3+} [15]. Therefore, the current work aims to highlight the role of Ti^{4+} partial substitution with Zr^{4+} ions on the crystallization tendency, lithium-ion conductivity, and microstructure of NASICON based glass-ceramics.

Table 1. Lattice parameters (a and c) and d-spacing taken from XRD patterns of glass-ceramics.

x (mole fraction)	a (nm)	c (nm)	d (nm)
0.0	0.8497	2.0964	0.36368
0.1	0.8507	2.1061	0.36469
0.2	0.8523	2.1171	0.36597
0.3	0.8536	2.2161	0.3669
0.4	0.8552	2.2261	0.38818

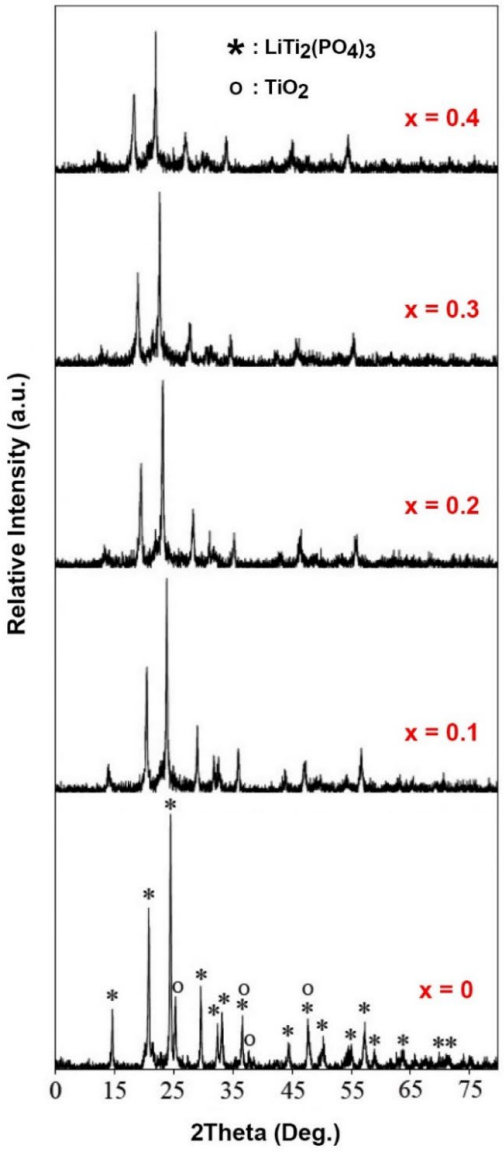

Fig. 2. Diffraction patterns of glass specimens undergone heat treatment at crystallization peak temperatures.

2. Experimental Procedures

Chemical compositions of starting glasses were chosen on the basis of $100[LiZr_xTi_{2-x}(PO_4)_3]$ and $5SiO_2$ (in mole ratio), where x = 0, 0.1, 02., 03., and 0.4. The base glass (x = 0) included 3.75 Li_2O, 40 TiO_2, 53.25 P_2O_5, and 3 SiO_2 (in wt%). Reagent grade chemicals of lithium carbonate, zirconium oxide, titanium oxide, phosphorous oxide, and silica were applied to prepare glass batch mixtures. The obtained mixtures were individually melted in an aluminum oxide crucible at 1450 °C for 3 h. Then, molten glasses were cast on steel sheets and rate. A one-step heat treatment procedure was applied to bulk pieces of glass to convert them into glass-ceramics. After

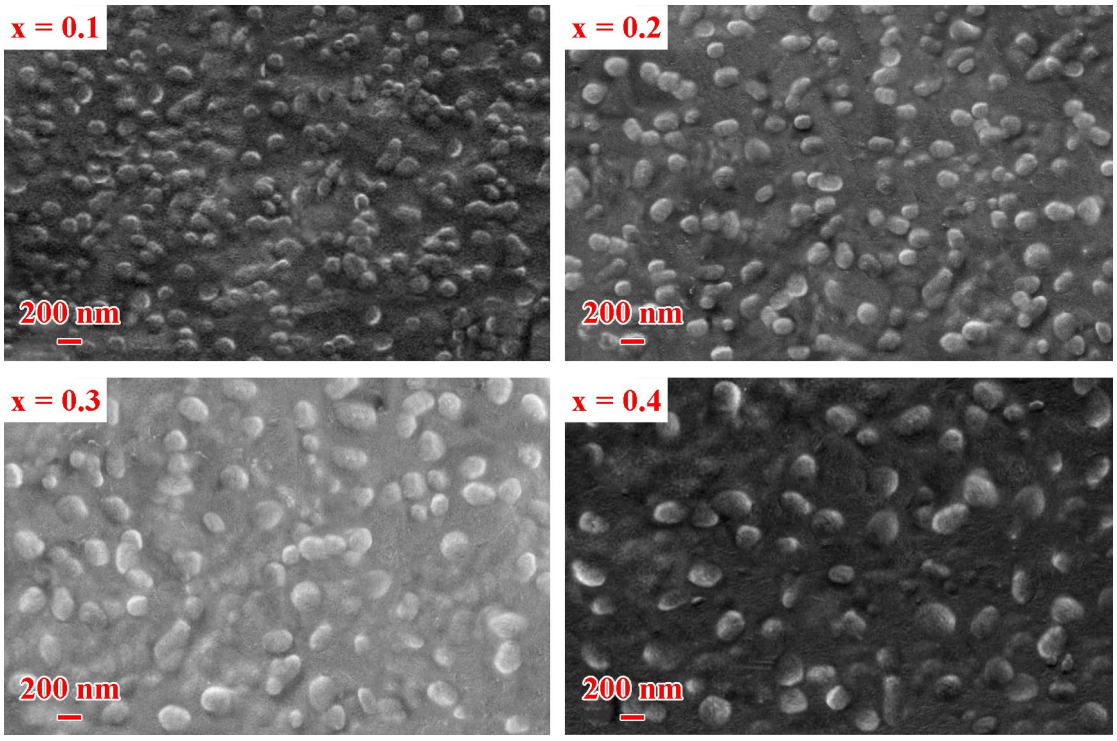

Fig. 3. SEM images of Zr containing glass-ceramics after 2 h heat treatment.

heat treatment, crystalline phases were recognized by the X-ray diffractometry instrument (Siemens D500) operating with Cu-K_α radiation. XRD analysis extracted the d-spacing of the main peak line using Xpert Highscore software. Lattice parameters (a and c) were also calculated according to the Rietveld refinement and applying MAUD software.

Microstructural features of glass-ceramics were analyzed by scanningelectron microscope (Sigma/VP, Zeiss). Before these observations, the glass-ceramic specimens were immersed in the dilute solution of hydrofluoric acid to be chemically etched. Afterward, they were coated by a thin layer of sputtered gold. The ionic conductivity of the fabricated glass-ceramics was measured by AC impedance spectroscopy (Solartron-1260) in the 0.1–10^7 Hz range of frequency. This measurement was conducted at 0–100 °C temperatures.

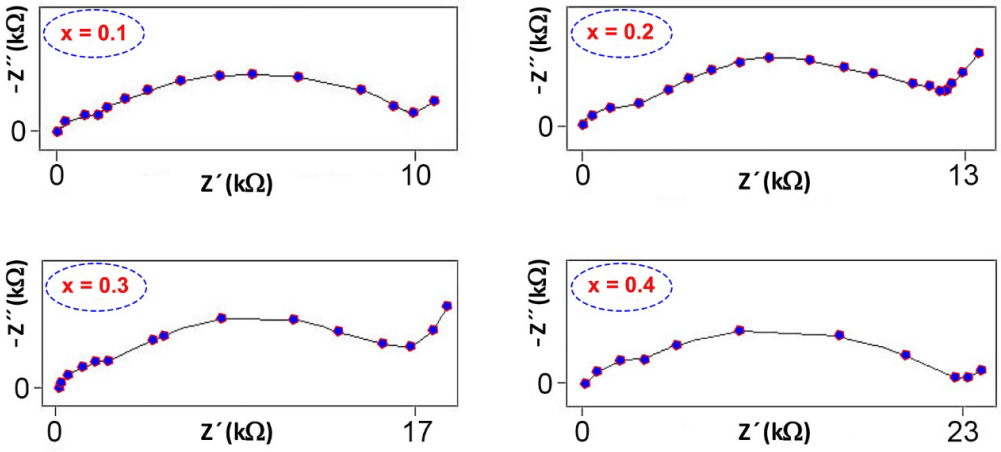

Fig. 4. Impedance plots of Zr containing glass-ceramics taken at room temperature.

Table 2. Ionic conductivity of glass-ceramics at room temperature. (σ_b: grain conductivity, σ_t: total conductivity).

x (mole fraction)	σ_b (S.cm^{-1})	σ_t (S.cm^{-1})
0	9.2×10^{-5}	3.04×10^{-5}
0.1	7.4×10^{-5}	1.8×10^{-5}
0.2	5.3×10^{-5}	1.4×10^{-5}
0.3	3.9×10^{-5}	1.02×10^{-5}
0.4	3×10^{-5}	0.78×10^{-5}

3. Results and discussion

Fig. 1 represents the DTA curves of the initial glasses. Referring to this figure, a single exothermic peak is detectable in each DTA curve related to the occurrence of crystallization in the studied glasses. It also implied that crystallization peaks shift to higher temperatures by further increasing Zr in the glass composition.

Fig. 2 indicates diffraction patterns of glass specimens after 2 h heat treatment at the crystallization peak temperature. Obviously, NASICON type ($LiTi_2(PO_4)_3$) and titanium oxide (TiO_2) are respectively present as the foremost and negligible crystalline phases in the base specimen (x = 0). It can be also observed that through the partial replacement of Ti by Zr in the glass composition and its further increase, the peak lines of titanium oxide have been omitted from the XRD patterns of Zr-bearing glass-ceramics. On the other hand, the intensity of the main peak lines of NASICON phase has been considerably declined contrary to the increased crystallization temperature. This means that by further replacement of Ti by Zr in the glass composition, the crystallinity of the relevant glass-ceramics has been gradually suppressed.

In order to examine the incorporation of Zr ions to the NASICON structure as a solid solution crystalline phase, lattice parameters (a and c), as well as the d-spacing of the strongest peak line in each XRD pattern of Fig. 2, were calculated according to the Rietveld refinement and applying MAUD software. These measurements have been shown in Table 1.

According to Table 1, by increase of Zr content in the glass composition, lattice parameters along with the d-spacing have been both increased confirming partial substitution of Ti ions by Zr ions in the structure of NASICON Phase. As a result, by the increase of Zr content from x = 0 to x = 0.4 the location of the strongest peak line of NASICON phase shifts from 24.47 to 22.98 ° (see Fig. 2).

In Fig. 3, SEM images of Zr-bearing glass-ceramics after 2 h heat treatment (at the crystallization peak temperature) have been illustrated. It could be observed that the crystalline phases have pseudo-spherical morphology. Moreover, crystallinity has been suppressed and microstructural coarsening happened with a further increase of Zr in the glass composition. Considering the decreasing trend of crystallinity in the Zr-containing glass-ceramics, it can be deduced that thermal energy has been consumed towards the growth of crystalline phases during heat treatment.

The impedance plots of Zr containing glass-ceramics recorded at 298 K can be observed in Fig. 4. Detection of one semi-circle in these plots confirms that there is a single conducting phase in the examined glass-ceramics. In each plot, total (R_t) and bulk resistance (R_b) are respectively achieved from the interception of the corresponding plot with the horizontal axis in low (right part of the semi-circle) and high (left part of the semi-circle) frequencies. Then, the total (σ_t) and bulk ionic conductivity (σ_b) conductivities can be obtained using Eq. 1:

$$\sigma = t/AR \quad (1)$$

where t, A, and R refer to the thickness, area and resistance of the specimen, respectively [16]. Table 2 summarizes these measurements.

It could be seen that further addition of Zr in the glass composition, gradually declines bulk and total ionic conductivity of relevant glass-ceramics. As a result, among the examined glass-ceramic specimens, the least values of bulk (3×10^{-5} S.cm^{-1}) and total ionic conductivity (0.78×10^{-5} S.cm^{-1}) were obtained for the specimen containing the highest amount of Zr (x = 0.4) in the glass composition.

Table 3. Total ionic conductivity of glass-ceramics at different temperatures (0, 25, 50, 75, and 100 °C).

x (mole fraction)	σ_t (S.cm^{-1}) 0 °C	σ_t (S.cm^{-1}) 25 °C	σ_t (S.cm^{-1}) 50 °C	σ_t (S.cm^{-1}) 75 °C	σ_t (S.cm^{-1}) 100 °C
0	11.1×10^{-6}	3.04×10^{-5}	6.12×10^{-5}	15.07×10^{-5}	2.74×10^{-4}
0.1	6.14×10^{-6}	1.8×10^{-5}	4.5×10^{-5}	10.02×10^{-5}	2.03×10^{-4}
0.2	4.37×10^{-6}	1.4×10^{-5}	3.6×10^{-5}	8.6×10^{-5}	1.77×10^{-4}
0.3	2.96×10^{-6}	1.02×10^{-5}	2.75×10^{-5}	6.77×10^{-5}	1.51×10^{-4}
0.4	2.09×10^{-6}	0.78×10^{-5}	2.23×10^{-5}	6.13×10^{-5}	1.3×10^{-4}

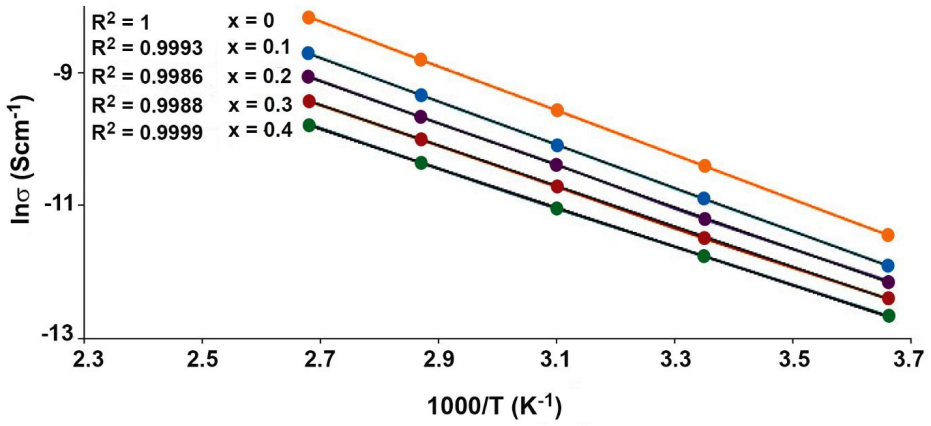

Fig. 5. Variation of ln σ_t versus 1/T for the examined glass-ceramic specimens.

In order to evaluate the activation energy of ionic conductivity, all glass-ceramic specimens were subjected to impedance spectroscopy at different temperatures (0, 25, 50, 75, 100 °C). Then, total conductivity was measured, separately for each specimen. Table 3 briefly shows these measurements.

According to Table 3, for each series of specimens, the temperature rise has led to a significant increase in total ionic conductivity. Afterward, the activation energy of ionic conductivity (E_a) was calculated based on Eq. 2:

$$\sigma_t = A \exp(-E_a/kT) \quad (2)$$

In this equation, A, k, and T are pre-exponential factor, Boltzmann constant, and temperature, respectively. Fig. 5 illustrates the variation of ln σ_t versus 1/T for all examined glass-ceramics.

From Fig. 5, the slope of each plot equals $-E_a/k$. Hence, the activation energies of ionic conductivity were simply calculated and summarized in Table 4.

It can be deduced that the addition of Zr to the parent glasses and its further increase has led to the gradual enhancement of E_a meaning that the chemical modification of parent glasses has negatively influenced the ionic conductivity of corresponded glass-ceramics. This result is in agreement with the findings of XRD analyses and microstructural observations.

Table 4. Activation energy of ionic conductivity of the glass-ceramics.

x (mole fraction)	E_a (kJ/mole)
0	27.91
0.1	29.61
0.2	31.44
0.3	33.2
0.4	35.14

4. Conclusions

- The base and Zr containing glass-ceramics were successfully prepared. In all fabricated glass-ceramics, lithium titanium phosphate crystallized as the main crystalline phase.
- Addition of Zr to the chemical composition of parent glasses considerably shifted crystallization temperature to higher temperatures.
- Further addition of Zr to the glass composition resulted in declined crystallinity as well as microstructural coarsening.
- The lowest bulk (3×10^{-5} Scm^{-1}) and total conductivity (0.78×10^{-5} Scm^{-1}) were obtained for x = 0.4 at ambient temperature.

CRediT authorship contribution statement

Parisa Goharian: Investigation, Formal Analysis, Methodology, Writing – original draft.

Alireza Aghaei: Supervision, Funding acquisition, Project administration, Resources.

Bijan Eftekhari Yekta: Supervision, Funding acquisition, Project administration, Resources.

Sara Banijamali: Writing – review & editing, Methodology, Validation, Data curation.

Data availability

The data underlying this article will be shared on reasonable request to the corresponding author.

Declaration of competing interest

The authors declare no competing interests.

Funding and acknowledgment

This project was financially supported by Materials and Energy Research Center (MERC, Iran) with project number of 381392050.

References

[1] Y. Yang, R. Wang, Z. Shen, Q. Yu, R. Xiong, W. Shen, Towards a safer lithium ion batteries: A critical review on cause, characteristics, warning and disposal strategy for thermal runaway, Adv. Appl. Energy. 11 (2023) 100146. https://doi.org/10.1016/j.adapen.2023.100146.

[2] F. Maisel, C. Neef, F. Marscheider-Weidemann, N.F. Nissen, A forecast on future raw material demand and recycling potential of lithium-ion batteries in electric vehicles, Resour. Conserv. Recy. 192 (2023) 106920. https://doi.org/10.1016/j.resconrec.2023.106920.

[3] S.V. Gaslov, M.S. Rublev, A.E. Biryukov, S.O. Kopytov, Virtual simulation of the operation of a lithium-ion battery as a part of a vehicle using ID complex model, Transport. Res. Procedia. 68 (2023) 906–916. https://doi.org/10.1016/j.trpro.2023.02.127.

[4] Z. Kou, C. Miao, Z. Wang, W. Xiao, Novel NASICON-type structural Li1.3Al0.3Ti1.7SixP5(3-0.8x)O12 solid electrolytes with improved ionic conductivity for lithium ion batteries, Solid State Ion. 343 (2019) 115090. https://doi.org/10.1016/j.ssi.2019.115090.

[5] H. Gan, W. Zhu, L. Zhang, Y. Jia, Zr doped NASICON-type LATP glass-ceramic as a super-thin coating onto deoxidized carbon wrapped CNT-S cathode for lithium-sulphur battery, Electrochim. Acta. 423 (2022) 140567. https://doi.org/10.1016/j.electacta.2022.140567.

[6] S. Jia, H. Akamatsu, G. Hasegawa, S. Ohno, K. Hayashi, Glass-ceramic route to NASICON-type NaxTi2(PO4)3 electrodes for Na-ion batteries, Ceram. Int. 48 (2022) 24758–24764. https://doi.org/10.1016/j.ceramint.2022.05.125.

[7] M.G. Moustafa, M.M. S. Sanad, M.Y. Hassaan, NASICON-type lithium iron germanium phosphate glass-ceramic nanocomposites as anode materials for lithium ion batteries, J. Alloys Compd. 845 (2020) 156338. https://doi.org/10.1016/j.jallcom.2020.156338.

[8] Y. Shao, G. Zhong, Y. Lu, L. Liu, C. Zhao, et al., A novel NASICON-based glass-ceramic composite electrolyte with enhanced Na-ion conductivity, Energy Storage Mater. 23 (2019) 514–521. https://doi.org/10.1016/j.ensm.2019.04.009.

[9] J.M. Valle, C. Huang, D. Tatke, J. Wolfenstine, Characterization of hot-pressed von Alpen type NASICON ceramic electrolytes, Solid State Ion. 369 (2021) 115712. https://doi.org/10.1016/j.ssi.2021.115712.

[10] S. Saffirio, M. Falco, G.B. Appectecchi, F. Smeacetto, C. Gerbaldi, Li1.4Al0.4Ge0.4Ti1.4(PO4)3 promising NASICON-structured glass-ceramic electrolyte for all solid state Li-based batteries: Unravelling the effect of diboron trioxide, J. Eur. Ceram. Soc. 42 (2022) 1023–1032. https://doi.org/10.1016/j.jeurceramsoc.2021.11.014.

[11] J.M. Naranjo-Balseca, C.S. Martinez-Cisneros, B. Pandit, A. Varez, High performance NASICON ceramic electrolytes produced by tape-casting and low temperature hot-pressing: Towards sustainable all-solid-state sodium batteries operating at room temperature, J. Eur. Ceram. Soc. 43 (2023) 4826–4836. https://doi.org/10.1016/j.jeurceramsoc.2023.04.008.

[12] R.P. Rao, C. Maohua, S. Adams, Preparation and characterization of Nasicon type Li ionic conductor, J. Solid State Electrochem. 16 (2012) 3349–3354. https://doi.org/10.1007/s10008-012-1780-x.

[13] P.Goharian, A. Aghaei, B. Eftekhari, S. Banijamali, Ionic conductivity and microstructural evaluatuion of Li2O-TiO2-P2O5-SiO2 glass-ceramics, Ceram. Int. 41 (2015) 1757–1763. https://doi.org/10.1016/j.ceramint.2014.09.121.

[14] B. Zarabian, B. Eftekhari Yekta, S. Banijamali, Crystallization behavior and ionjic conductivity of NASICON type glass-ceramics containing different amounts of B2O3, Synth. Sinter. 3 (2023) 1419. https://doi.org/10.53063/synsint.2023.31141.

[15] P.Goharian, B. Eftekhari, A. Aghaei, S. Banijamali, Lithium-ion conducting glass-ceramics in the system Li2O-TiO2-P2O5-Cr2O3-SiO2, J. Non-Cryst. Solids. 409 (2015) 120–125. https://doi.org/10.1016/j.jnoncrysol.2014.11.016.

[16] A. Chandra, A. Bhatt, A. Chandra, Ion conduction in superionic glassy electrolytes: An overview, J. Mater. Sci. Tech. 29 (2013) 193–208. https://doi.org/10.1016/j.jmst.2013.01.005.